PS Effects of Porosity Models on Thermal History in Geohistory Models*

Alton A. Brown[1]

Search and Discovery Article #41392 (2014)**
Posted July 24, 2014

*Adapted from poster presentation given at 2014 AAPG Annual Convention and Exhibition, Houston, Texas, April 6-9, 2014

[1]Consultant, Richardson, Texas, USA (altonabrown@yahoo.com)

Abstract

Paleotemperature modeled by geohistory simulation is controlled by ancient surface temperature, heat flow (HF), and thermal conductivity (TC). The problems associated with estimating grain TC are well recognized by the literature, but the influence of porosity uncertainty on TC and paleotemperature is not so well recognized. In commercial geohistory software, porosity is calculated as an exponential function of maximum burial depth or effective stress, but porosity loss is actually a function of effective stress and time (by cementation and mineralogical conversion). Porosity models calibrated to current porosity may underestimate ancient porosity. Lower porosity causes higher TC, so paleo temperatures estimated from a modeled HF will be underestimated. This effect can be substantial for mudrocks. One solution is to modify the porosity models to better match observed physical processes. Transient sandstone and limestone porosity loss can be modeled using published algorithms. For mudrocks, the most robust approach is to divide porosity into free water and bound water. Model the free water loss using the standard compaction equilibrium approach. Model the transient bound-water loss by clay reactions. Bound water content is related to the cation exchange capacity (CEC) of the rock. The CEC and bound water will decrease significantly, as smectite converts to illite. As CEC decreases, total porosity decreases. Smectite-illite conversion kinetics are available in the literature. Unfortunately, transient porosity models cannot be implemented into the current commercial geohistory programs, but they can be incorporated into research software. Transient models reduce porosity with time, so models calibrated to modern porosity correctly estimate current temperatures and modern HF but underestimate paleotemperatures where HF is constant. If modern porosity is estimated from literature mechanical compaction models and strata are old, modeled modern TC and modern HF may be underestimated. As an empirical short-term solution for commercial software users, porosity models can be calibrated to modern porosity-depth, and the effects of lower paleo TC can be compensated by increasing paleo HF and surface temperature.

We do this anyway when HF history is modified to match thermal indicators. Thus, geodynamic interpretations of higher paleo HF derived by fitting HF history to thermal indicators using current porosity-depth models may be invalid.

Effects of Porosity Models on Thermal History in Geohistory Models

Alton A. Brown, Consultant, Richardson, TX altonabrown@yahoo.com

Abstract

Paleo temperature modeled by geohistory simulation is controlled by ancient surface temperature, heat flow (HF), and thermal conductivity (TC). The problems associated with estimating grain TC are well recognized by the literature, but the influence of porosity uncertainty on TC and paleo temperature is not so well recognized.

In commercial geohistory software, porosity is calculated as an exponential function of maximum burial depth or effective stress, but porosity loss is actually a function of effective stress and time (by cementation and mineralogical conversion). Porosity models calibrated to current porosity may underestimate ancient porosity. Lower porosity causes higher TC, so paleo temperatures estimated from a modeled HF will be underestimated. This effect can be substantial for mudrocks.

One solution is to modify the porosity models to better match observed physical processes. Transient sandstone and limestone porosity loss can be modeled using published algorithms. For mudrocks, the most robust approach is to divide porosity into free water and bound water. Model the free water loss using the standard compaction equilibrium approach. Model the transient bound-water loss by clay reactions. Bound water content is related to the cation exchange capacity (CEC) of the rock. The CEC and bound water will decrease significantly as smectite converts to illite. As CEC decreases, total porosity decreases. Smectite-illite conversion kinetics are available in the literature. Unfortunately, transient porosity models cannot be implemented in the current commercial geohistory programs, but they can be incorporated into research software.

Transient models reduce porosity with time, so models calibrated to modern porosity correctly estimate current temperatures and modern HF but underestimate paleotemperatures where HF is constant. If modern porosity is estimated from literature mechanical compaction models and strata are old, modeled modern TC and modern HF may be underestimated.

As an empirical short-term solution for commercial software users, porosity models can be calibrated to modern porosity-depth, and the effects of lower paleo TC can be compensated by increasing paleo HF and surface temperature. We do this anyway when HF history is modified to match thermal indicators. Thus, geodynamic interpretations of higher paleo HF derived by fitting HF history to thermal indicators using current porosity-depth models may be invalid.

Introduction

A key parameter for basin thermal history analysis is the thermal conductivity of the sediment. All commercial geohistory models estimate ancient bulk thermal conductivities from mineral thermal conductivity and porosity using a geometric mixing law (see below). Previous studies have stressed the importance of correct mineral thermal conductivity and mixing model (e.g., Midttømme, et al., 1997). The purpose of this poster is to demonstrate the influence of the porosity model on ancient subsurface temperatures.

As a layer compacts with burial, porosity decreases and layer thermal conductivity increases. The vast majority of geohistory models (and all commercial geohistory software of which I am aware) assume that porosity is an exponential function of effective stress or equivalent depth. This is certainly an incorrect assumption for carbonates and sandstones, because porosity is reduced by cementation (e.g., Schmoker 1984, Lander and Walderhaug, 1999, Brown 1987). Cementation is a rate process that involves time. It is almost certain that mudrocks also undergo transient porosity loss. Porosity in older mudrocks is less than that predicted from drained consolidation tests, and porosity in old mudrocks is less than porosity in young mudrocks exposed to similar maximum effective stresses.

If porosity loss is a transient process, and if maximum-effective-stress porosity models are used and calibrated to modern porosity, modeled paleo-porosity will be less than actual paleo-porosity. If porosity is underestimated, thermal conductivity is overestimated and the model will underestimate ancient temperatures. Underestimated temperatures cause underestimated thermal maturity indicators and delayed onset of petroleum generation.

The purpose of this poster to evaluate the magnitude of the porosity effect on ancient burial temperatures and to suggest both long- and short-term approaches to better estimate ancient temperatures in geohistory models.

- First, simple-minded end member cases based on empirical data will be modeled to demonstrate that reasonable porosity differences between porosity models based on empirical data can cause significant temperature differences.
- A foreland basin subsidence of a shale basin will then be modeled with a preliminary transient mudrock porosity model.
- Implications for tectonic subsidence interpretation and ancient heat flow estimation will be briefly discussed.
- Finally, several short-term solutions are suggested for simple cases of interest to the practical basin modeler.

There are no answers in this poster, only quantification of problems and suggested hypotheses for future work directions.

Mudrock Porosity Effects on Temperature

To test the potential effects of non-transient porosity models on ancient mudrock thermal conductivity and maximum temperature, the thermal conductivities and temperatures calculated assuming the Athy porosity trend are compared to those calculated assuming the composite Gulf of Mexico Cenozoic trend discussed below (Figure 6). We are interested in temperature as a function of depth at a time soon after a Paleozoic-aged foreland shale basin was deposited.

The following scenario is tested. A sedimentary section of Paleozoic age that is entirely mudrock has a present-day porosity-depth trend that follows the Athy trend (Figure 6). The porosity-depth trend soon after burial is unknown. Two porosity-depth trends are modeled as end members of possible porosity distribution immediately after the foreland subsidence pulse. One porosity trend is the same as the Athy trend observed today. This assumes that porosity is a function of depth alone and not of time. The second porosity trend is the composite Gulf of Mexico Cenozoic trend, (GOM on Figure 6). This assumes that porosity is transient. Porosity followed the GOM trend soon after deposition, but it now follows the Athy trend due to porosity loss during the last several hundred million years of burial. We model the thermal conductivity and temperature developed by the two porosity models using the same surface temperature and heat flow.

Because of its higher porosity, the GOM trend has thermal conductivity lower than that of the Athy trend (Figure 7). Compaction also affects paleo-depth of all strata. If porosity is less today than it was in the past, horizons must have been buried deeper in the past than they are today, even without erosion. The depth of equivalent horizons are estimated from equivalent cumulative solidity (meters of solid rock below the surface). Cumulative solidity is not affected by compaction models. Two horizons of the same age were arbitrarily selected (Figure 8). The depth difference due to compaction for horizons 1 and 2 are 270 m and 472 m, respectively.

Temperatures were calculated from the surface temperature, heat flow, and thermal conductivity profile assuming steady, conductive heat flow (Figure 9). Temperatures using the GOM model are higher than those at the same depth in the Athy model. At depths of 2400 m and 4400 m, temperature differences are 12°C and 20°C, respectively. Temperature differences at horizons 1 and 2 are 20°C and 33°C, respectively.

If mudrocks did have transient porosity and the modern porosity trend as assumed, then modeled ancient heat flow in the steady model would have to be increased to match the temperatures in the transient model. Heat flow assuming constant Athy porosity-depth has to be increased from 70 mW/m^2 to 90 mW/m^2 to match the paleo temperatures in the transient model.

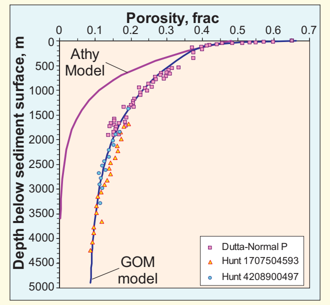

Figure 6. Modeled mudrock porosity trends. One is a exponential trend following the Athy data. The gulf of Mexico trend (GOM) is compared to the Dutta et al. (2009) and selected Hunt et al. (1998) data.

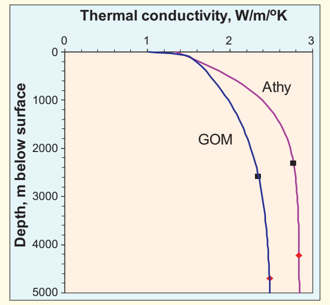

Figure 7. Mudrock bulk thermal conductivity vs. depth for porosity models in Figure 6. Thermal conductivity is the geometric average of a matrix TC of 2.98 W/m/oK (30% quartz; 70% clay) and water-filled porosity.

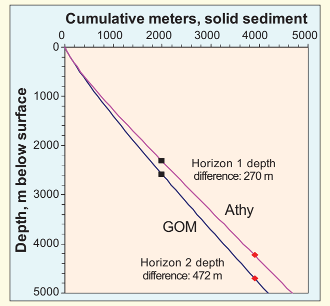

Figure 8. Cumulative solidity vs. depth for porosity models in Figure 6. Cumulative solidity for a time horizon in a well is the same for all porosity models. Symbols are the depths of the two selected horizons.

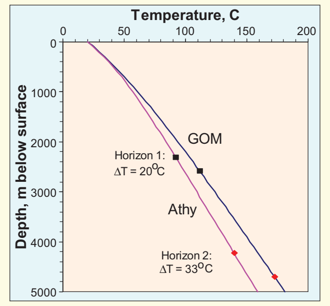

Figure 9. Temperature vs. depth for porosity models in Figure 6 assuming a heat flow of 70 mW/m^2 and 20°C surface temperature. Symbols are depths of two equivalent time horizons at maximum burial.

Limestone Porosity Effects on Temperature

To test maximum possible temperature effects of the porosity model on a limestone basin, Paleozoic porosity trends were compared to Cenozoic trends. Assume a foreland basin with a rapid Paleozoic depositional pulse followed by no additional burial. The strata are entirely limestone. We are interested in the temperatures at the end of the foreland depositional pulse using two porosity models: a constant porosity-depth trend based on the low-porosity Williston basin data, and a transient trend where early porosity-depth is assumed to follow the South Florida basin data before late cementation alters the porosity trend to that following the Williston Basin trend.

The questions are how much hotter the transient model would be, how much of that temperature difference is caused by conductivity changes to a given depth, and how much temperature difference is caused by deeper paleoburial of horizons under the high porosity model.

Thermal conductivities vs. depth were calculated from the porosity and thermal conductivities of calcite and water using geometric averaging (Figure 11). Porosities of the two porosity trends are estimated as a function of depth using the exponential fits of porosity (see below). Temperatures were calculated from the surface temperature, heat flow, the two thermal conductivity profiles, and assumed steady conductive heat flow. Surface temperature and heat flow in both models are 20°C and 0.07 W/m^2, respectively. The cumulative solidity calculated from the porosity curves were used to compare depths of the same horizons in the two models.

As expected, higher temperature develops in the high porosity model due both to lower thermal conductivity at depth and deeper maximum burial due to its greater porosity. A horizon with a solidity of 2000m was 27°C hotter and about 370 m deeper at end of foreland basin deposition using the transient model (Figure 12). Conductivity difference down to a depth near 2000m accounts for about 20°C temperature difference. Thus, most of the modeled temperature difference between the same horizon in the two models is caused by the conductivity effect rather than deeper burial.

The horizon with a solidity of 4000m is about 33°C hotter and 478 m deeper at the end of foreland basin deposition if the transient porosity is assumed. About 23°C of this temperature difference is caused by conductivity differences in the overlying section (Figure 12).

The limestone models have the same general results as the mudrock models; if anything, temperature differences in limestone basins are more sensitive to transient vs. static compaction models than shale basins. If transient compaction occurs at approximately the magnitude modeled here, then temperatures soon after deposition are substantially underestimated by models assuming constant porosity-depth relationships. If the sedimentation pattern has a foreland basin style, then maximum temperature (and thus the thermal maturity patterns) will develop soon after the end of the foreland basin pulse.

Because less data are available for average limestone porosity against depth as a function of age and burial history, timing of limestone porosity loss is less certain than that of mudrocks. There is overwhelming evidence for transient compaction of limestones, and the transient effect appears to be large. However, the kinetics of this process is still not well documented.

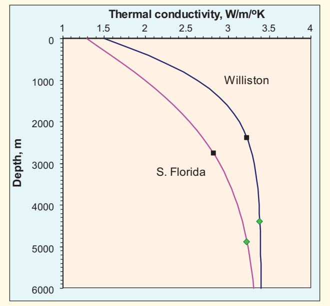

Figure 11. Limestone bulk thermal conductivity vs. depth for porosity models in Figure 10. Bulk thermal conductivity is the geometric average of a matrix TC of 3.4 W/m/°K (100% calcite) and water-filled porosity. Porosity models are identified by the name of the basins where the porosity-depth models were derived.

Figure 12. Temperature vs. depth for porosity models in Figure 10 assuming a heat flow of 70 mW/m^2 and 20°C surface temperature. Symbols are depths of two equivalent time horizons (cumulative solidity of 2000 and 4000 m).

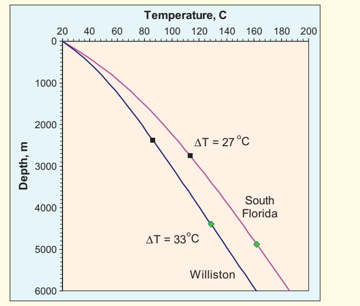

Mineral Thermal Conductivities Used Here

Mineral or fluid	TC, W/m/°K	Density, g/cc	Citation
Quartz	7.7	2.65	Horai 1971
Calcite	3.4	2.71	Horai 1971
Dolomite	5.4	2.88	Horai 1971
illite	1.85	2.75	Brigaud and Vasseur, 1989
Smectite	1.88	2.2	Brigaud and Vasseur, 1989
Kaolinite	2.6	2.42	Brigaud and Vasseur, 1989
K-feldspar	2.4	2.57	Horai 1971
Albite	2.2	2.62	Horai 1971
Anhydrite	5	2.96	Horai 1971
Gypsum	1.3	2.32	Horai 1971
water	0.6	1	generalized, many sources

Averaging Equations

Geometric Average
$$BTC = \left(\sum_{i=1}^{p} TC_i^{\,v_i}\right)^{1-\phi} TC_f^{\,\phi}$$
Averaging matrix and porosity in an isotropic random medium where ϕ is the porosity, TC is the thermal conductivities of each of p mineral species and of a single fluid f. Mineral volume fractions (V_i) sum to 1.

Harmonic Average
$$BTC = \frac{\sum_{i=1}^{n} L_i}{\sum_{i=1}^{n} \frac{L_i}{TC_i}} = \frac{\sum_{i=1}^{n} L_i}{\sum_{i=1}^{n} TR_i}$$
Averaging TC of heat flow normal to infinite layers, where L_i are thickness of layers and TC_i are thermal conductivities of layers.

Power Average
$$BTC = \left(\frac{1}{n}\sum_{i=1}^{n} TC_i^{\,p}\right)^{1/p}$$
Generalized average that allows upscaling intermediate between arithmetic, geometric, and harmonic averages by changing the value of p from 1 to -1. The n are proportional to the volume of components, and TC_i is the thermal conductivity of component i.

Background: Thermal Conductivity Models

Thermal Conductivity

Thermal conductivity relates a thermal gradient to heat flow under steady, conductive heat transfer. It is a tensor that is treated as a vector in multidimensional heat-flow models and as a scalar in 1-D (well) geohistory models. In sediments, thermal conductivity is controlled by the mineralogy, porosity, and fabric. The thermal conductivities of minerals and water used for models presented here are shown on the table at right.

Upscaling Sample Thermal Conductivity

Estimating bulk rock thermal conductivity is an upscaling problem similar to upscaling other flow properties such as permeability. Heat flows through simple composite media can be calculated by simple averaging methods. Arithmetic mean approximates flow parallel to layers in a layered medium. Harmonic mean approximates series flow across layers in a layered medium. Geometric mean approximates heat flow through a random composite medium with isotropic elements. Models for heat flow through rocks with fabrics intermediate between layered and random fabrics can be approximated by the generalized power average (see equations at left).

Geometric averaging is used for estimating the thermal conductivity of porous rocks in all geohistory programs of which I am aware. The geometric volumetric average of mineral and fluid thermal conductivities has been found empirically to approximate the thermal conductivity of multi-mineral rocks and porous rock where the rock has an isotropic fabric (e.g., Fuchs et al. 2013, Brigaud and Vasseur 1989; Hartmann et al. 2005). Other, more complex models give similar results over the range of porosity and thermal conductivity ratios seen in most sedimentary rocks (Fuchs et al. 2013), but these models require other data not readily available for subsurface strata.

Model Thermal Conductivity

Heat flow across sedimentary layers is a series flow problem which is universally modeled in geohistory programs as the harmonic average of the layer thermal conductivities. Thermal resistance (thickness/thermal conductivity) is more suited for series heat-flow problems because thermal resistance is additive in series heat-flow. In this study, temperatures are calculated from the sum of the thermal resistance from the surface, surface temperature, and heat flow.

Mudrock Thermal Conductivity

There is considerable scatter to thermal conductivity measurements in mudrocks. Older studies report bulk thermal conductivities for mudrocks that are significantly lower than thermal conductivity determined by the geometric average of the water-saturated porosity and mineral constituents. In fact, Blackwell and Steele (1989) and Carter et al. (1998) propose that mudrocks are better fit by a constant, low thermal conductivity than geometric mixing models.

More recent lab measurements of the thermal conductivity of consolidated mudrock and other argillaceous sediment using the optical scanning technique are in the 1.5 to 4 W/m/°K range (Figure 1). The optical scanning thermal conductivities are in approximate agreement with geometric averaging models (Hartmann et al. 2005, Norden and Forster 2006, Fuchs and Forster 2010, Fuchs et al. 2013, Fuchs and Forster 2014). The mudrock TC estimates are consistent with geometric averages of matrix minerals and porosity (Figure 2). Inversion of closer-spaced stabilized well temperature data give in situ thermal conductivities similar to thermal conductivities measured by the optical scanning technique (e.g., Hartmann et al. 2005; Fuchs and Forster 2010).

The optical scanning thermal conductivity data generally validate the way thermal conductivities have been modeled in geohistory models using geometric averages of porosity and a matrix thermal conductivity estimated from mineralogical composition. Some or most of the problems with mudrock thermal conductivity measurement and estimation reported in the older literature may be due to measurement error rather than poor fit to a geometric mixing model or exceptionally low mudrock thermal conductivities. Fuchs et al. (2013) discuss possible sources of these errors. In this poster, mudrock thermal conductivities are calculated using geometric average of porosity and mineral constituents.

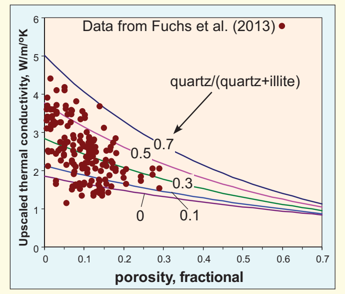

Figure 1. Measured mudrock thermal conductivities (filled circles) compared to geometric average of quartz-illite-porosity mixtures. Data from Fuchs et al. (2013); trends are calculated from matrix TC values listed at left.

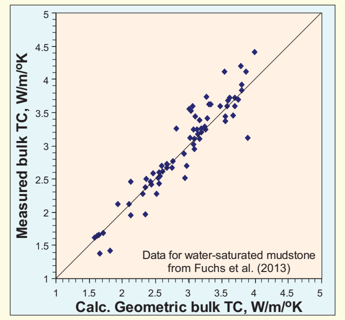

Figure 2. Comparison of bulk thermal conductivity calculated from mineral properties and porosity by geometric average with measured bulk thermal conductivity of water-saturated samples. Data from Fuchs et al. (2013).

Mudrock Porosity vs. Depth

Geohistory Porosity Models

Porosity is typically modeled as an exponential function decreasing with either increasing maximum burial depth, maximum effective stress, or maximum equivalent depth (depth corrected for excess pressure). There are theoretical reasons for exponential porosity decrease with depth (e.g., Bahr, et al., 2001), but in most cases, the exponential porosity trends are chosen for empirical reasons. Modeled porosity either does not increase or increases very slightly with exhumation or secondary geopressure development.

Cenozoic Porosity Trends

The focus of this study is porosity trends in normal-pressured rocks. Data from the Gulf of Mexico normal pressured mudrocks will be used to illustrate Cenozoic mudrock porosity trends. In normal pressured settings, depth strongly correlates with vertical effective stress, so porosity in a well can be related empirically to either with equal statistical validity.

Dutta et al. (2009) porosity data collected from normal pressured zones show two porosity trends with depth (Figure 3). Porosity at burial less than about 100 m below sea floor (about 1 MPa vertical effective stress) decreases rapidly with depth similar to that documented by Hamilton (1977) and consolidation tests. Porosity at deeper depth decreases at a slower rate as a concave-downwards function of depth and effective stress. Each trend can be fit by an exponential function, but the combined trend cannot be accurately represented by a single exponential function.

Revil and Cathles (2001) interpret an almost linear trend of porosity against vertical effective stress over the range of effective stress that they investigated (Figure 3). Their data follow a trend similar to that of the Dutta data, only offset to a slightly higher porosity at equivalent effective stress. This offset could be caused by the younger age of the sediment investigated by Revil and Cathles (2001). Alternately, it might be an artifact of the density assigned to the unlogged shallow sediment that is used to calculate the vertical effective stress for deeper strata.

Hunt et al. (1998) evaluate cuttings-density data collected by Amoco many years ago (Figure 4). These data show a shallow linear decrease in porosity with increasing depth that changes to a relatively constant porosity at greater depth. Porosity in normal-pressured zones in many of these wells actually can be fit by an exponential trend that asymptotically approaches a porosity (ϕ_1) greater than zero (i.e., $\phi = \phi_1 + \phi_2 \exp(-c^*depth)$. The temperature at which porosity approaches this asymptote decreases as stratigraphic age increases (Hunt et al. 1998).

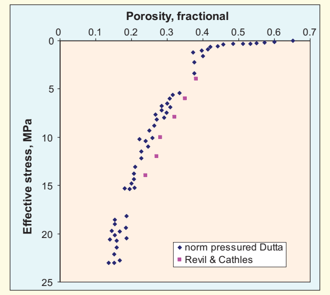

Figure 3. Gulf of Mexico normal-pressured mudrock porosity as a function of maximum effective stress. Data from normal-pressured wells in Green Canyon area shown in Figure 4 in Dutta et al. (2009) and from Plio-Pleistocene strata, Block 330 field area (Revil and Cathles 2001).

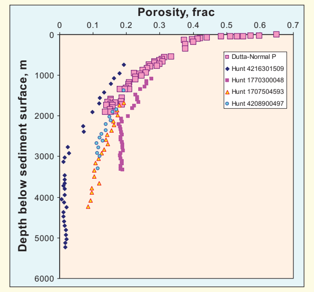

Figure 4. Gulf of Mexico normal-pressured mudrock porosity as a function of depth below sediment surface. Data from Hunt et al. (1998, identified by well API number) compared to normal pressure data in Dutta et al. (2009).

A generalized Gulf of Mexico (GOM) Cenozoic normal-pressured porosity trend can be constructed for modeling purposes by combining data from the younger, normal pressured Cenozoic strata in the Hunt et al. (1998) wells with data from the normal pressured wells in Dutta et al (2009). Porosity is described as a function of depth by ϕ = 0.34exp(-0.0008D) + 0.25exp(-0.03D)+0.08 (Figure 6). D is depth in meters below sediment surface at maximum burial. The first term is the porosity loss with depth in the deeper part of the well, the second term is the exponential porosity loss in the upper hundred meters or so, and the final term is the porosity offset.

Paleozoic Porosity Trend

There are few published mudrock porosity compilations for Paleozoic mudrocks. The best data are those of Athy (1930; Figure 5), which are based on core Archimedes densities and porosities. Porosities at depth are much lower than porosities of younger strata at equivalent depth, such as those of Dutta et al. (2009; Figure 5). The low measured porosities in Athy's data are consistent with the fast transit times of moderate- to deeply-buried, organically lean Paleozoic shales throughout the midcontinent The low porosities at depth are sometimes less than the bound-water porosity expected from the clay abundance in similar rocks. This indicates that cementation has reduced porosity. The Athy trend is exponential: ϕ = 0.48exp(-0.00146*D), where D is depth in meters below sediment surface at maximum burial.

Figure 5. Northern Oklahoma Pennsylvanian mudrock porosity (Athy 1930) compared to shallow, Gulf of Mexico mudrock porosity from Dutta et al. (2009).

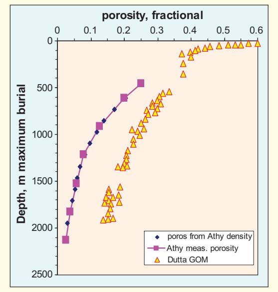

Limestone Porosity vs. Depth

Cenozoic-Cretaceous Porosity - Depth

Average porosities are higher in Cenozoic and Cretaceous limestone than in early Mesozoic and Paleozoic strata at equivalent maximum burial depth (Schmoker 1984). The best documented porosity trends for younger strata are those for the South Florida basin (Schmoker and Halley 1982). Figure 10 shows Schmoker and Halley limestone porosities averaged by 1000 ft (300 m) intervals plotted against current depth (blue diamonds, Fig. 10). Data can be fit by an exponential function of burial depth: ϕ = 0.6exp(-0.0006D). Model explained variance (R^2) is 0.96.

Paleozoic Porosity vs. Depth

The porosity vs. depth data of Brown (1997) from Mississippian-aged limestones of the US Williston basin were used as an example (Magenta squares, Figure 10). These data were fit with an exponential porosity vs. depth relation: ϕ = 0.47exp(-0.0012D). Model explained variance (R^2) is 0.94. From my own experience, lower Paleozoic (Cambro-Ordovician) limestones have much lower porosity than these Mississippian limestones.

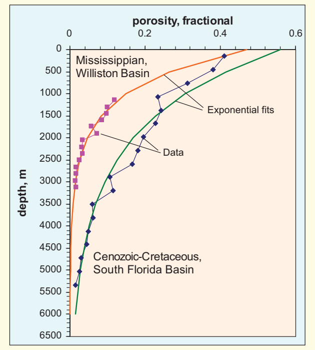

Figure 10. Comparison of Cenozoic-Cretaceous limestone porosity trend against Mississippian limestone porosity trend with depth. Solid lines are exponential fits to the data; symbols connected by short lines are the average data.

Presented at AAPG ANNUAL MEETING, Houston, 2014

Effects of Porosity Models on Thermal History in Geohistory Models

Alton A. Brown, Consultant, Richardson, TX altonabrown@yahoo.com

Mudrock Transient Geohistory Model

Preliminary Transient Mudrock Compaction Model

Basic mechanisms for transient compaction of mudrock over the time scale of interest have not been widely discussed or published. In absence of a published model to guide evaluation of transient compaction, a preliminary, partially calibrated, mudrock transient model was developed. The model is described below. To summarize, mudrock porosity is divided into free water and bound water. Free water is lost by mechanical compaction, whereas bound water is lost by clay mineral diagenesis and quartz cementation.

A simple, Excel-based geohistory program was written that could use this transient model during burial and uplift to calculate time and temperature. Thermal conductivity is calculated from the geometric average of mineral TC and porosity. Temperature in all layers and times are calculated from steady heat conduction using input heat flow and surface temperature. Tectonic subsidence is calculated from water depth and depth of basement through time.

Model Test

A foreland-basin style of tectonic subsidence was modeled for a 100% mudrock section. A uniform solidity accumulation rate of 200 m of porosity-free mudrock per million years was deposited for 16 million years on basement. Subsidence abruptly stops and is followed by 280 million years with no deposition or erosion. Sediment in all layers has the mineral content and thermal properties listed in Table 1 below. Heat flow and surface temperature are constant at values listed in Table 1. Heat flow follows a steady conductive model. Water depth is assumed zero at all times.

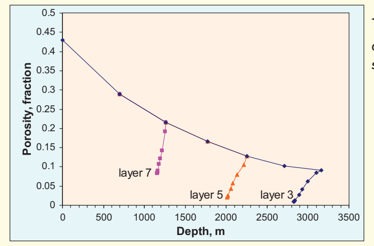

Figure 17a. Porosity as a function of burial depth with time for three selected layers.

The preliminary transient compaction model developed below was calibrated by this geohistory model. Modeled porosity at 284 Ma was calibrated to the Cenozoic Gulf of Mexico porosity trend (Figure 15). Modeled modern porosity was calibrated to the Athy porosity-depth trend (Figure 15). These calibrations are based on the assumption that average mudrock depositional composition of the Paleozoic mudrocks is identical to those of the Cenozoic Gulf of Mexico.

Model Results

During deposition, all layers show similar porosity-depth trends because subsidence rate is constant (Figure 17). Porosity loss during this time period could be modeled by a traditional porosity-effective stress model.

After deposition stops, transient models become necessary. Porosity continues to decrease (Figure 13, 17). Stratal burial depth decreases with time since end of deposition (Figure 13). This reverses the porosity vs. depth trend through time for a layer (Figure 17). As porosity and depth decrease with time since sedimentation stopped, temperatures for horizons decrease (Figure 14).

Because porosity decreases while heat flow is kept constant, the temperature - depth trend decreases with time (Figure 16). At the base of the model, temperature immediately after deposition stopped (284 Ma) was about 25°C hotter than it is today (Figure 16). Layers were buried deeper in the past, so part of the cooling since maximum burial is caused by difference in burial depth.

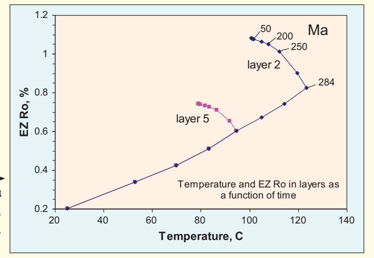

Figure 17b. Modeled EZ Ro as a function of temperature for two layers. Key ages are labeled for layer 2 results.

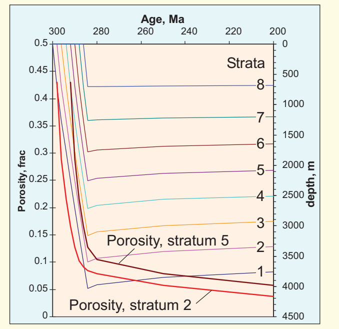

Figure 13. Geohistory burial plot showing depth of strata and porosity of selected strata with age before present. Porosity loss continues after sedimentation stops. Deep strata become shallower with time after deposition due to continued compaction of overlying strata.

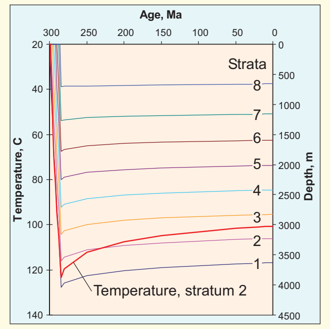

Figure 14. Geohistory burial plot showing depth of strata and temperature near the base of the model with age before present. Temperature decreases with time due to decreasing porosity and depth.

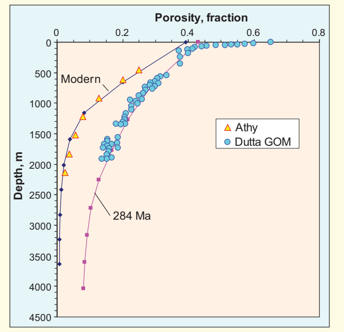

Figure 15. Modeled porosity vs. depth plotted for the two calibration times (284 Ma and 0 Ma) compared to Athy (1930) and Dutta et al. (2009) porosity data.

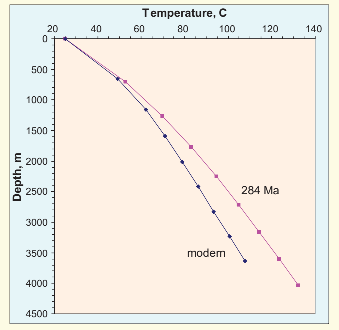

Figure 16. Temperature vs. depth at a time soon after deposition stops (284 Ma) and after over 280 million years of non-deposition (modern). Symbols correspond to horizons on the model, so temperature differences between the horizons can be compared.

Geodynamic Implications

Tectonic subsidence was calculated for the model described by figures 10-13 (Figure 19). Tectonic subsidence curves calculated for the transient porosity model show significant tectonic uplift after termination of foreland subsidence which was not input into the model. This is an artifact. Basement has to have a tectonic uplift to offset the subsidence that would occur from porosity reduction due to the constant sea level assumption for the model. In the absence of tectonic subsidence or uplift, accommodation space would be created for deposition by transient compaction.

Tectonic subsidence modeled using a constant porosity-depth relationship for a foreland basin with transient compaction will not be correct. The weight and thickness of sediment will not be estimated correctly if porosity is not correctly characterized. Tectonic subsidence must also be added to account for the accommodation space created by transient compaction. If tectonic subsidence curves are used to estimate a beta factor for an earlier thermal subsidence section, the beta factor will not be correctly estimated. Predicted heat-flow changes related to thermal subsidence will be in error. Magnitude of this effect has not been calculated for a rift setting, and it might be small.

Figure 19. Tectonic subsidence calculated from transient model of Figs. 13-16 using both air (heavy black line) and water (heavy red line). Thin lines are depths to horizons assuming zero water depth and no sea-level changes.

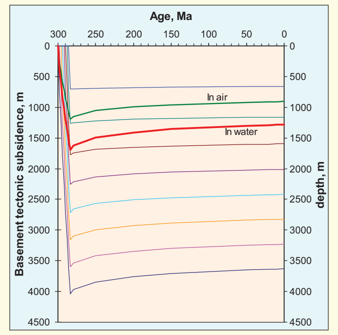

Layer Lithological Heterogeneity

Upscaling Layer Thermal Conductivity

Most layers in geohistory models are composite, because bedding is on all scales. Does the layer-average clay content and assumed homogeneous lithology of the layer give a substantially different upscaled thermal conductivity than a layered medium?

Synthetic models were used to test bedding effects on layer thermal gradient. Models consist of sandstones with 10, 50, and 70 volume% mudstone beds. Porosity of the sandstones were fixed at either 5% or 30%, and mudstone porosity varied. Thermal conductivity is calculated for the bedded medium using the harmonic average of the porous sandstone and porous mudstone layers. The thermal conductivity of a homogeneous rock with equivalent average mudrock content and average porosity was calculated from the geometric average of the rock components and porosity. To maximize heterogeneity, the thermal conductivities of the sandstone matrix and mudstone matrix were set at 7.7 and 2.8 W/m/°K. Results are plotted as a ratio of the thermal conductivity upscaled as beds to that upscaled as a homogeneous rock.

Results

All bedded models have upscaled thermal conductivities within 85% of the homogeneous assumption (Figure 18). Where mudrock porosity is similar to sandstone porosity, upscaled thermal conductivity differences are negligible. Even where porosities are significantly different, the temperature error introduced by geometric upscaling of matrix thermal conductivity will not be large if a heterogeneous geohistory layer is thin.

Thick intervals comprising multiple lithologies in near equal abundance should be assigned to separate geohistory model layers to avoid incorrect thermal conductivity upscaling.

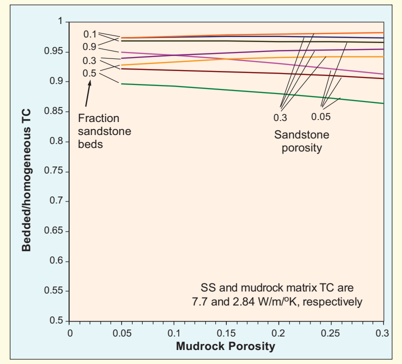

Figure 18. Ratio of thermal conductivity of a bedded medium to that of a homogeneous medium for media with different mudstone and porosity fractions as a function of the mudstone porosity.

Conclusions

Chemical processes continue in buried sediment after deposition stops. Porosity decreases with chemical reaction, so porosity is a transient phenomenon rather than a simple function of maximum effective stress or burial. Transient compaction is not modeled by any of the commercial geohistory programs, so effects of simplification of porosity to a function of effective stress has not been evaluated. This poster investigates the magnitude of thermal effects resulting from different porosity assumptions.

In general, constant porosity-effective stress models calibrated to modern well porosity cause the model to underestimate maximum burial depth and temperature. Porosity affects temperature and thermal maturity in two ways. Higher porosity in overlying strata increases maximum burial depth. Higher porosity also decreases thermal conductivity. Under assumed constant heat flow, lower thermal conductivity causes higher temperatures. Transient compaction with its higher porosity earlier in the burial history can therefore cause ancient temperatures to be higher than calculated from geohistory models using constant porosity-effective stress models.

If it is assumed that porosity vs. depth in Paleozoic strata soon after their deposition is similar to porosity vs. depth in Cenozoic passive margins, then temperature of strata at depths in the oil window will be underestimated by 20° to 30°C. Most of this temperature difference is the result of overestimated thermal conductivity, but underestimated maximum burial is also significant.

A preliminary time-transient mudrock compaction model was developed to demonstrate that reasonable diagenetic mechanisms can cause the observed porosity-depth difference between Cenozoic and Late Paleozoic mudrock strata. Modeled mudrock porosity is lost by mechanical compaction, decreasing bound-water porosity due to smectite-illite transformation, and quartz cementation with a nucleation kinetics control.

Despite their incomplete porosity models, geohistory models can be made to match thermal maturity data by increasing paleo heat flow to compensate for higher thermal conductivity in the simulated burial history. However, geodynamic interpretations from models using constant porosity-effective stress models are suspect. Tectonic subsidence curves will be wrong, and magnitudes of elevated heat flow are uncertain and suspect. This results in uncertain timing of petroleum generation in Paleozoic basins even where modeled thermal maturity matches observed values.

Mudrock Model Parameters

Total Porosity

At all depths and time, total porosity is the sum of the free-water porosity and the bound-water porosity. Free-water porosity is reduced only by mechanical compaction. Bound-water porosity is reduced by clay diagenesis and quartz cementation.

Free-Water Porosity

Free-water porosity is reduced entirely by mechanical compaction. At any time k, free-water porosity is an exponential function of effective stress:

$$\phi_{f,k} = \phi_{fi}\, exp(-c\sigma_{vm,k})$$

Where $\phi_{f,k}$ is free-water porosity, ϕ_{fi} is the initial free-water porosity, c is the consolidation coefficient per MPa, and $\sigma_{vm,k}$ is maximum vertical effective stress in MPa up to time k.

Bound-Water Porosity

Initial bound water is controlled by the fractions of clay minerals. Initial mineralogy is the same in all layers (Table 1). Bound water (ϕ_b) at all depths is estimated from dry weight fractions (F) of clays using the following equation (Modified from Dewan 1983):

$$\phi_b = \frac{0.8(F_{smectite} + 0.25F_{illite} + 0.2F_{chlorite} + 0.04F_{kaolin})}{1 + 0.8(F_{smectite} + 0.25F_{illite} + 0.2F_{chlorite} + 0.04F_{kaolin})}$$

Bound water changes by two processes: clay diagenesis and quartz cementation. Fractions of illite and smectite change with burial due to smectite conversion to illite. As the clay type changes, the bound water changes. The smectite-illite transition was modeled using parallel, first-order kinetics modified from Wei et al. (1996). Table 2 compares the kinetics of Wei et al. and the kinetic parameters used here.

Because this is a first-order reaction, the bound-water porosity lost at each step by smectite conversion to illite is proportional to the bound-water porosity at the previous step, composite rate constant (K, a function of temperature, T), and the duration of the step:

$$f_{i-s,k} = \frac{\phi_{i-s,k}}{\phi_{i-s,k-1}} = exp(-K_t(t_k - t_{k-1}))$$

Quartz Cementation

Cementation causes porosity loss from the bound water porosity fraction. Because mudrock pores are small, cementation is modeled as a nucleation-controlled process. Pores are sufficiently small that the odds of a nuclei forming within a pore is small within a unit of time, but once nucleated, the cement crystal can rapidly occlude the pore. Porosity loss by nucleation control can be described by the following differential equation and rate loss per time interval:

$$\frac{d\phi}{dt} = -6JD^2\phi \qquad f_{c,k} = \frac{\phi_{c,k}}{\phi_{c,k-1}} = exp(-6JD^2(t_k - t_{k-1}))$$

where $f_{c,k}$ is the fractional porosity loss by cementation during step k, D is the pore diameter, ϕ is porosity, t is time, and J is the nucleation rate in nuclei/cm^2/s.

Nucleation is heterogeneous on the mineral surfaces, but it is treated here by classical homogeneous nucleation theory. J is:

$$J = A\exp\left(\frac{-B}{[\ln(S)]^2}\right)$$

Where S is the degree of supersaturation and A and B are two empirical constants. Supersaturation in the burial environment can be related to the effective stress using the following:

$$S = \exp\frac{\sigma_n V}{RT}$$

where V is the molar volume, R is the gas constant, T is absolute temperature, and σ_n is the effective stress normal to the surface of interest.

Total Porosity Loss

Total porosity (ϕ_t) is the sum of the free-water (ϕ_f) and bound-water (ϕ_b) porosities. Free porosity is reduced only by mechanical compaction. Bound water is reduced by clay diagenesis and cementation. Total bound-water porosity reduction is the product of bound-water porosity of the previous step, fractional decrease of bound-water porosity during that time step caused by quartz cementation, and by fractional decrease of bound-water porosity lost by smectite conversion to illite:

$$\phi_{b,k} = f_{c,k}\, f_{i-s,k}\, \phi_{b,k-1}$$

Table 1: Model parameters

Initial mineralogy: Smectite: 0.25, Illite: 0.05; Kaolinite: 0.1; Chlorite: 0.05; Quartz: 0.5; Calcite: 0.5
Mechanical parameters: ϕ_{fi} = 0.25; c = 0.12.
Cementation parameters: initial bound water porosity: 0.18. 1 micron pore diameter; V: 22.67 cc/mole; A: 300,000 nuclei/cm^2/My; B: 0.01
Thermal properties (all times and layers): Heat flow: 70 mW/m^2; Matrix thermal conductivity: 4 W/m/°K; Water thermal conductivity: 0.6 W/m/°K; Surface temperature: 25°C

Table 2: Smectite-Illite kinetic parameters. Pre-exponential term is 0.00086 per second for all activation energies. Wei et al. weight fractions are normalized to 0.8 to account for their 0.2 weight fraction of unreactive smectite.

Activation energy, cal/mole	Renormalized Wei et al. wt. fractions	Weight fractions used here
11000	0.0030	0
12000	0.0080	0
13000	0.0080	0
14000	0.0082	0
15000	0.0164	0
16000	0.0083	0
17000	0.1041	0.115
18000	0.5261	0.55
19000	0.0726	0.075
20000	0.0087	0.055
21000	0.0088	0.055
22000	0.0156	0.05
23000	0.0087	0.05
24000	0.0035	0.05

Discussion

General Results

The porosity-depth and porosity-effective stress relationships used in the current generation of 1-D geohistory models have the potential to significantly underestimate porosity for ancient strata because they fail to account for transient compaction related to chemical processes. Basins with underestimated porosity also underestimate maximum burial depth of horizons and their maximum temperatures. Stress-related compaction, petroleum generation, vitrinite reflectance, etc. will be underestimated by geohistory models that underestimate temperature and maximum stress.

Although the evidence for time-transient compaction is compelling, especially for sandstone and carbonate lithologies, the actual controls on time-transient compaction are not well understood, so the actual influence of transient behavior cannot be assessed, only effects contingent on a particular porosity models. If porosity in Paleozoic strata soon after deposition is similar to that of Cenozoic strata, temperature effects are quite significant.

Perhaps the reason transient compaction has not been well studied for geohistory applications is the ease with which thermal indicator data can be matched by altering ancient temperatures in geohistory models. To compensate for the poorly estimated ancient thermal conductivity by the current generation of exponential porosity-depth models, simply increase past heat flow or add more eroded deposition. Models of nearby wells with similar stratigraphic columns using the revised heat flow, eroded deposition history, and simple porosity-maximum effective stress relationships will in many cases correctly predict thermal maturity indicators in the test wells. Timing remains an issue even where the model is adjusted to match thermal maturity indicators. The heat flow and erosion history needed to match thermal indicators is not unique. Timing of generation in older strata is therefore uncertain even in models that match the thermal indicator data.

Subtle Effects of Transient Compaction

- Compaction after thermal maturity indicators are set by an earlier maximum temperature will steepen the indicator depth gradient. The steeper maturity indicator gradient can be (incorrectly) interpreted as evidence for higher thermal gradient in the past.
- Porosity-depth trends assigned using model default porosity based on generalized lithology may lead to incorrect modern porosity in geohistory models and therefore incorrect assessment of modern heat flow. Porosity models used in geohistory programs should be compared to actual well porosities if at all possible to correctly assess modern heat flow.
- Tectonic subsidence curves created for Paleozoic basins are suspect until implications of transient compaction on sediment load are evaluated. Where tectonic subsidence curves are used to interpret beta factors in ancient rifts, the beta factors may not be correctly estimated, so basement heat flow due to rifting and thermal subsidence may not be correctly estimated.

Modeling Strategies

Current commercial geohistory programs cannot include effects of transient compaction on temperature structure. Three general strategies can be used to get around this limitation:

- Business as usual. Ignore the compaction problem, and assign elevated ancient heat flow history where necessary to match thermal maturity data. This is by far the most expeditious strategy where all study wells have similar lithologies and general burial histories. However, timing of generation will be suspect in geohistory models of Paleozoic strata, because multiple heat-flow histories can explain modern thermal maturity trends in a well.
- If Paleozoic subsidence has a foreland basin pattern, apply a exponential porosity-depth trend for the lithology of interest based on Cenozoic data. Run the model using modern heat flows up to about 30 million years after the foreland depositional pulse stops. Temperature at maximum burial will be the major control on thermal maturity, and it is best predicted from porosity distributions at the time of maximum burial. This only works where later burial is significantly less than maximum burial at the end of foreland basin deposition.
- Include transient compaction models in the next generation of geohistory software. This will require a better understanding of transient compaction mechanisms in different sediment types. Processes controlling sandstone transient compaction (porosity loss) are fairly well understood, at least to the first order needed for burial history analysis (e.g., Lander and Walderhaug 1999). Conceptual models for limestone compaction are available in the literature (e.g., Brown 1987). However, there are still major problems with converting pressure-dissolution reaction rates to porosity loss in systems dominated by dissolution at stylolites. Diagenetic studies of mudrocks have not coupled the diagenetic reactions to porosity. Therefore, mudrocks that have the greatest gap in understanding transient compaction.

Acknowledgments

I thank Pangaea Resources, Ltd (Australia) for presenting this interesting problem.

Older versions of carbonate transient porosity concepts were developed at the ARCO research lab in Plano prior to 2000. Preliminary transient compaction concepts and ideas were discussed many years ago with Jeff Corrigan, Zhiyong He, Steve Franks, and Bob Loucks.

I thank Michael Jones, Graeme Beardsmore, and Herve van Baelen for discussions about mudrock thermal conductivity. These discussions did not always come to a consensus, but they did drive a literature search for better quality data.

Porosity-depth models were run on older versions of Genesis and PetroMod 1D express in addition to the model described here. Developers of these programs are gratefully acknowledged.

This poster is dedicated to the memory of Sal Bloch, a true petroleum geologist and pioneer in reservoir quality prediction.

References

Athy, L. F., 1930, Density, porosity, and compaction of sedimentary rocks: AAPG Bulletin, v. 14#1, p. 1 – 24. '

Bahr, D. B., E. W. H. Hutton, J. P.M. Syvitski, and L. F. Pratson, 2001, Exponential approximations to compacted sediment porosity profiles: Computers & Geosciences v. 27 p. 691–700.

Blackwell, D. D., and J. L. Steele, 1989, Thermal conductivity of sedimentary rocks: measurement and significance, in N. D. Naeser and T. H. McCulloh, eds., Thermal history of sedimentary basins - methods and case histories: New York, Springer-Verlag, p. 13–36.

Brigaud, F., and G. Vasseur, 1989, Mineralogy, porosity, and fluid control on thermal conductivity of sedimentary rocks: Geophysical Journal, v. 98, p. 525-542.

Brown, A. A., 1987, Mechanisms of pressure solution in limestones: applications to numerical models of porosity loss: SEPM Annual midyear meeting Abstracts, v. 4, p. 10 (Austin, TX meeting).

Brown, A. A., 1997, Porosity variation in carbonates as a function of depth: Mississippian Madison Group, Williston Basin, in: Reservoir Quality Prediction in Sandstones and Carbonates: AAPG Memoir 69, p. 29 - 46.

Carter, L. S., S. A. Kelley, D. D. Blackwell, and N. D. Naeser, 1998, Heat flow and thermal history of the Anadarko Basin, Oklahoma: AAPG Bulletin, V. 82, No. 2 p. 291–316.

Dutta, T. G. Mavko, T. Mukerji, And T. Lane, 2009, Compaction trends for shale and clean sandstone in shallow sediments, Gulf of Mexico: The Leading Edge May 2009, p. 590 – 596.

Fuchs, S. and A. Forster, 2010, Rock thermal conductivity of Mesozoic geothermal aquifers in the Northeast German Basin: Chemie der Erde – Geochemistry, v. 70, Supplement 3, August 2010, P. 13–22.

Fuchs, S., Förster, A., 2014, Well-log based prediction of thermal conductivity of sedimentary successions: examples from the North German Basin: Geophysical Journal International – v. 196, #1, p. 291-311.

Fuchs, S., Schütz, F., Förster, H. J., Förster, A., 2013, Evaluation of common mixing models for calculating bulk thermal conductivity of sedimentary rocks: Correction charts and new conversion equations: Geothermics, v. 47, p. 40-52.

Hamilton, E. L., 1976, Variations of density and porosity with depth in deep-sea sediments: Journal of Sedimentary Petrology, v. 46, p. 280-300.

Hartmann, A., V. Rath, and C. Clauser, 2005, Thermal conductivity from core and well log data: International Journal of Rock Mechanics & Mining Sciences, v. 42, p. 1042–1055.

Horai, K., 1971, Thermal conductivity of rock-forming minerals: J. Geophysical. Research., v. 76, #5, p. 1278-1308.

Hunt, J. M., J. K. Whelan, L. B. Eglinton, and L. M. Cathles, 1998, Relation of Shale Porosities, Gas Generation, and Compaction to Deep Overpressures in the U.S. Gulf Coast, Chapter 5 in: Abnormal Pressures in Hydrocarbon Environments, B.E. Law, G.F. Ulmishek, and V.I. Slavin, eds. AAPG Memoir 70, p. 87 – 104.

Lander, R. H. and O. Walderhaug, 1999, Predicting porosity through simulating sandstone compaction and quartz cementation: AAPG Bulletin, v. 83, # 3, p. 433–449.

Midttømme, K., E. Roaldset, and P. Aagaard, 1997, Thermal conductivities of argillaceous sediments, in: Modern Geophysics in Engineering Geology, Engineering Geology Special Publications, D. M. McCann, M. Eddleston, P. J. Fenning, G. M. Reeves, eds. , v. 12, Geological Society, London, 1997, p. 355-363.

Norden B. and A. Forster, 2006, Thermal conductivity and radiogenic heat production of sedimentary and magmatic rocks in the Northeast German Basin: AAPG Bulletin, v. 90, no. 6, p. 939–962.

Revil, A., L. M. Cathles, 2001, The porosity-depth Pattern defined by 40 wells in South Eugene Island Block 330 area, and its relation to pore pressure, fluid leakage, and seal migration: in: Petroleum Systems of Deep-Water Basins: Global and Gulf of Mexico Experience, R. H. Fillon, N. C. Rosen, and P. Weimer, eds.: GCSSEPM 21st Bob F. Perkins Research Conference, p. 687-712.

Schmoker, J. W. , 1984, Empirical relation between carbonate porosity and thermal maturity: an approach to regional porosity prediction, AAPG Bull., v. 68, p. 1697-1703.

Schmoker, J. W. and R. B. Halley, 1982, Carbonate porosity vs. depth: a predictable relation for South Florida: AAPG Bulletin v. 66, p. 2561-2570.

Wei, H., E. Roaldset, and M. Bjoroy, 1996, Parallel reaction kinetics of smectite to illite conversion: Clay Minerals v. 31, p. 365-376.